Supporting Information

V-shaped nematogens with the "Magic bent angle"

Jens Seltmann,[b] Kathrin Müller[b], Susanne Klein,[c] Matthias Lehmann[a,b]*

[a]*Institute of Organic Chemistry, University of Würzburg, Am Hubland, 97074 Würzburg, Germany*
[b]*Institute of Chemistry, Chemnitz University of Technology, Straße der Nationen 62, 09111 Chemnitz, Germany*
[c]*HP Labs, Long Down Avenue, Stoke Gifford, Bristol BS34 8QZ, United Kingdom*

Acknowledgement: We thank the DFG for the financial support (LE 1571/2-1), H. Meier, A. Oehlhof and N. Hanold (University of Mainz) for FD MS and elemental analysis data and J. Gutmann and M. Bach for the available X-Ray equipment at the Max-Planck-Institute of Polymer Research, Mainz.

Content

1) Experimental details and analytical data of V-shaped compounds

Chemicals were obtained from Acros and Sigma-Aldrich and used as received. The synthesis of compounds **2-4** was described previously.[1,2] The target compounds were obtained by analogous procedures, detailed in reference.[1] Column chromatography was carried out on silica 60 (Merck, mesh 70–230). PFT ^{1}H and ^{13}C NMR spectra were recorded in $CDCl_3$ with a Varian Oxford 400 MHz spectrometer with the residual solvent signal at 7.26 ppm as a reference. Mass spectra were obtained on a Finnigan MAT95 (FD MS). Elemental analysis was carried out in the microanalytical laboratory at the University of Mainz. POM observations were made with a Zeiss Axioscop 40 equipped with a Linkam THMS600 hot stage. DSC was performed using a Perkin Elmer Pyris 1.

LC Cell assembly: Optically flat ITO (IndiumTinOxid) glass (Merck) was spin coated on the ITO side with the planar polyimide Nissan 130 (Nissan Chemicals). The film was first soft baked on a hot plate at 90°C for 1 min and then hard backed in a 180° degree oven for 1 hour. The cured film was rubbed using a custom made rubbing machine and cleaned with Isopropanol afterwards. The cells where assembled into antiparallel cells using 23 (cell(1) and 50 µm (cell (2)) thick mylar film as spacer. Antiparallel means that the rubbing directions of

[1] M. Lehmann, J. Seltmann, *Beilstein J. Org. Chem.* **2009**, *5*, 73.
[2] M. Lehmann, J. Seltmann, A. A. Auer, E. Prochnow, U. Bendikt, *J. Mater. Chem.* **2009**, *19*, 1978.

top and bottom substrate are opposite which should give a nematic liquid crystal a constant pretilt of 2° to 4° depending on the liquid crystal. The cells were then filled capillary.

Quantum mechanical calculations were performed at in vacuo DFT level of theory, by employing the combination of B3LYP functional and 6-311g(d,p) basis set. All the calculations were done with the Gaussian 09 package.[3]
X-Ray diffraction measurements were carried out on aligned samples in glass capillaries of 1.5 mm diameter. The nematic phases were aligned in a magnetic field (1T) upon cooling from the isotropic to the nematic phase. The WAXS measurements were performed by using a standard copper anode (2.2 kW) source with pinhole collimation equipped with a X-ray mirror (Osmic typ CMF15-sCu6) and a Bruker detector (High-star) with 1024 x 1024 pixels. The diffraction data were calibrated by using silver behenate as a calibration standard.[4] The X-ray patterns were evaluated using the datasqueeze software (http://www.datasqueezesoftware.com/).

General Procedure for the synthesis of terminal alkynes 5-7

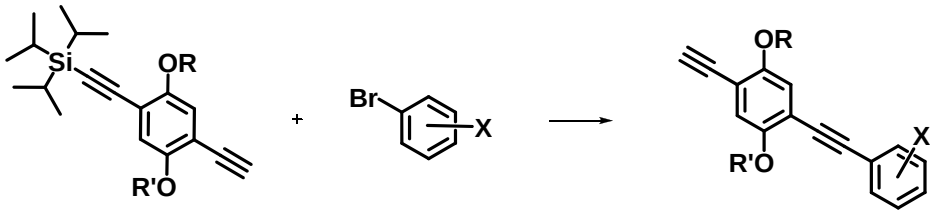

	R,R'
8a	Hexyl
b	Heptyl,Pentyl

	R,R'	X
5	Hexyl	*p*-CN
6	Hexyl	*m*-CN
7	Heptyl,Pentyl	*m*-CN

Scheme S1. Synthesis of the shape persistent arm building blocks **5-7**.

A mixture of 1.0 eq of **8a,b** 1.0 eq. of 3-bromobenzonitrile or 4-bromobenzonitrile, 0.1 eq of $Pd(PPh_3)_4$ and 0.05 eq of CuI in 50 ml piperidine is stirred for 1 h at 65 °C. Afterwards the solvent is removed *in vacuo* and the cross coupling products are isolated by column chromatography using a mixture of EtOAc/hexane = 50/1. These products are treated with 1.5 eq of TBAF in 40 ml THF and are stirred for 1 h at rt. After removing the solvent *in vacuo* the terminal alkynes **5-7** are purified by column chromatography with a mixture of EtOAc/hexane = 40/1. The experimental data of **8a**[5],**b**[6] and **5**[5],**6**[7] are described in literature.

1-(heptyloxy)-5-[(3-cyanophenyl)ethynyl]-2-ethynyl-4-(pentyloxy)benzene (7): yellow solid; melting point: 70 °C; **^{1}H NMR** (400 MHz, $CDCl_3$): δ 0.89 (t, 3H, CH_3, ^3J = 7.3); 0.93 (t, 3H, CH_3, ^3J = 7.4); 1.26 - 1.57 (m, 12H, CH_2); 1.78 - 1.88 (m, 4H, CH_2); 3.36 (s, 1H, C≡C H); 4.00 (t, 2H, OCH_2, ^3J = 6.4); 4.01 (t, 2H, OCH_2, ^3J = 6.6); 6.98 (s, 1H, CH); 6.99 (s, 1H, CH); 7.47 (m, 1H, CH); 7.60 (m, 1H, CH); 7.72 (m, 1H, CH); 7.79 (m, 1H, CH). **^{13}C NMR** (100 MHz, $CDCl_3$): δ 14.3 (CH_3); 22.6, 22.7, 26.0, 28.4, 29.1, 29.2, 29.3, 31.9 (CH_2); 69.7, 69.8(OCH_2); 79.9, 82.9, 88.4, 92.3 (C≡C); 113.0, 113.5, 113.6 (C_q); 116.9, 117.7 (C_t); 118.2, 125.2 (C_q); 129.4, 131.5, 134.9, 135.7 (C_t); 153.7, 154.2 (C_q).

---

[3] M. J. Frisch, et al. GAUSSIAN 09 (Revision A.01), Gaussian, Inc., Wallingford, CT, 2009.
[4] T. C. Huang, H. Toraya, T. N. Blanton, J. Wu, *J. Appl. Crystallogr.*, 1993, **26**, 180.
[5] M. Lehmann, J. Levin, *Mol. Cryst. Liq. Cryst.* **2004**, *411*, 273.
[6] J. Seltmann, M. Lehmann, *Liq. Cryst.* **2011**, *38,* 407.
[7] M. Lehmann, C. Köhn, H. Kresse, Z. Vakhovskaya, *Chem. Commun.* **2008**, 1768.

General Procedure for the synthesis of V-shaped mesogens 1 and 2

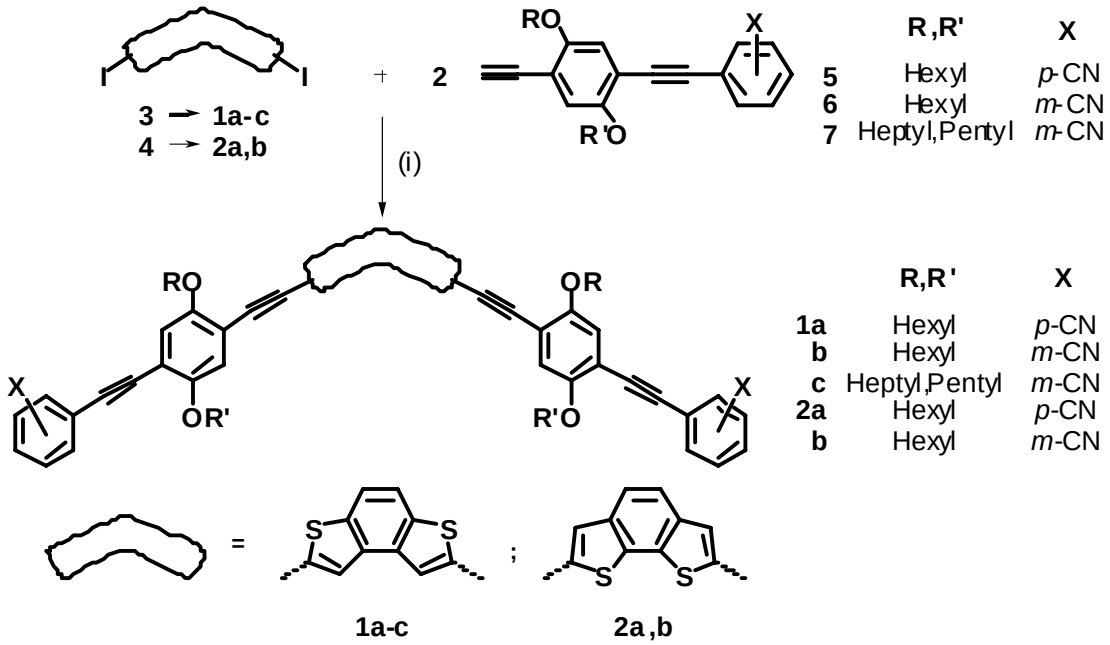

Scheme S2. Synthesis of the V-shaped mesogens **1** and **2**.

General procedure for synthesis of V-shaped mesogens **1** and **2**. A mixture of 1.0 eq of benzodithiophene core units **3** or **4**, 1.0 eq of the corresponding terminal alkynes **5-7**, 0.4 eq of $Pd(PPh_3)_4$ and 0.2 eq of CuI in 40 ml piperidine is stirred for 1 h at 40 °C. Afterwards the solvent is removed *in vacuo* and the products are isolated as yellow solids by means of column chromatography using a mixture of hexane/EtOAc = 20/1.

2,7-bis-{4-[4-(4-cyanophenylethynyl)-2,5-bis-(hexyloxy)phenyl]ethynylphenyl}benzo[1,2-b:4,3-b']dithiophene (1a): **^{1}H NMR** (400 MHz, $CDCl_3$): δ 0.90 (t, 6H, CH_3, ^3J = 6.9); 0.92 (t, 6H, CH_3, ^3J = 7.2); 1.30 - 1.46 (m, 16H, CH_2); 1.48 - 1.64 (m, 8H, CH_2); 1.80 - 1.93 (m, 8H, CH_2); 4.06 (t, 8H, OCH_2, ^3J = 6.4); 7.03 (s, 2H, CH); 7.05 (s, 2H, CH); 7.62 (8H, AA'BB'); 7.66 (s, 2H, CH); 7.82 (s, 2H, CH); **^{13}C NMR** (100 MHz, $CDCl_3$): δ 14.0, 14.1 (CH_3); 22.6, 22.7, 25.7, 25.8, 29.2, 29.3, 31.56, 31.62 (CH_2); 69.6, 69.7 (OCH_2); 88.7, 90.5, 92.1, 93.4 (C≡C); 111.5, 113.3, 114.3 (C_q); 116.5, 116.9 (C_t); 118.5 (C_q); 199.4 (C_t); 124.1 (C_q); 126.5 (C_t); 128.4 (C_q); 131.98, 132.05 (C_t); 134.0, 137.7, 153.7, 154.9 (C_q). **EA** [%]: $C_{68}H_{68}N_2O_4S_2$ Calc. for C 78.43, H 6.58, N 2.69, S 6.16 Found C 78.16, H 6.62, N 3.02, S 5.93; **FD-MS:** *m/z* [%]: 1040.6 (100, M^+); 1041.6 (78, $[M+1]^+$).

2,7-bis-{4-[4-(3-cyanophenylethynyl)-2,5-bis(hexyloxy)phenyl]ethynylphenyl}benzo[1,2-b:4,3-b']dithiophene (1b): **^{1}H NMR** (400 MHz, $CDCl_3$): δ 0.90 (t, 6H, CH_3, ^3J = 6.3); 0.92 (t, 6H, CH_3, ^3J = 6.3); 1.32 - 1.46 (m, 16H, CH_2); 1.50 - 1.64 (m, 8H, CH_2); 1.83 - 1.94 (m, 8H, CH_2); 4.057 (t, 4H, OCH_2, ^3J = 6.2); 4.063 (t, 4H, OCH_2, ^3J = 6.0); 7.03 (s, 2H, CH); 7.05 (s, 2H, CH); 7.48 (m, 2H, CH); 7.61 (m, 2H, CH); 7.74 (m, 2H, CH); 7.76 (s, 2H, CH); 7.80 (m, 2H, CH); 7.83 (s, 2H, CH); **^{13}C NMR** (100 MHz, $CDCl_3$): δ 14.2, 14.3 (CH_3); 22.8, 22.9, 25.9, 29.4, 29.5, 31.7, 31.8 (CH_2); 69.7, 69.8 (OCH_2); 88.6, 88.8, 92.2, 92.7 (C≡C); 113.1, 113.5, 114.1 (C_q); 116.6, 117.0 (C_t); 118.3 (C_q); 119.5 (C_t); 124.2, 125.2 (C_q); 126.7, 129.4, 131.6 (C_t); 134.2 (C_q); 135.0, 135.7 (C_t); 137.8, 153.7, 154.0 (C_q). **EA** [%]: $C_{68}H_{68}N_2O_4S_2$ Calc. for C 78.43, H 6.58, N 2.69, S 6.16 Found C 78.30, H 6.60, N 2.80, S 5.93; **FD-MS:** *m/z* [%]: 1040.6 (100, M^+); 1041.6 (61, $[M+1]^+$).

2,7-bis-{4-[4-(3-cyanophenylethynyl)-2-(heptyloxy)-5-(pentyloxy)phenyl]ethynylphenyl} benzo-[1,2-b:4,3-b']dithiophene (1c): **^{1}H NMR** (400 MHz, $CDCl_3$): δ 0.88 (t, 6H, CH_3, ^3J = 7.0); 0.95 (t, 6H, CH_3, ^3J = 7.2); 1.29 - 1.50 (m, 16H, CH_2); 1.56 (m, 8H, CH_2); 1.88 (m, 8H, CH_2); 4.056 (t, 4H, OCH_2, ^3J = 6.4); 4.061 (t, 4H, OCH_2, ^3J = 6.4); 7.03 (s, 2H, CH); 7.05 (s, 2H, CH); 7.48 (m, 2H, CH); 7.60 (m, 2H, CH); 7.74 (m, 2H, CH); 7.75 (s, 2H, CH); 7.81 (m, 2H, CH); 7.83 (s, 2H, CH); **^{13}C NMR** (100 MHz, $CDCl_3$): δ 14.3 (CH_3); 22.6, 22.8, 26.2, 28.4, 29.1, 29.3, 29.5, 32.0 (CH_2); 69.7, 69.8 (OCH_2); 88.6, 88.7, 92.2, 92.7 (C≡C); 113.0, 113.5, 114.1 (C_q); 116.5, 117.0 (C_t); 118.3 (C_q); 119.5 (C_t); 124.2, 125.2 (C_q); 126.7, 129.4, 131.5 (C_t); 134.1 (C_q); 135.0, 135.7 (C_t); 137.8, 153.8, 154.0 (C_q). **EA** [%]: $C_{68}H_{68}N_2O_4S_2$ Calc. for C 78.43, H 6.58, N 2.69, S 6.16 Found C 78.14, H 6.34, N 2.85, S 6.01; **FD-MS:** *m/z* [%]: 1040.8 (100, M^+); 1041.8 (78, $[M+1]^+$).

2,7-bis-{4-[4-(4-cyanophenylethynyl)-2,5-bis(hexyloxy)phenyl]ethynylphenyl}benzo[2,1-b:3,4-b']dithiophene (2a): **^{1}H NMR** (400 MHz, $CDCl_3$): δ 0.90 (t, 6H, CH_3, ^3J = 6.8); 0.93 (t, 6H, CH_3, ^3J = 6.4); 1.30 - 1.46 (m, 16H, CH_2); 1.50 - 1.64 (m, 8H, CH_2); 1.80 - 1.93 (m, 8H, CH_2); 4.05 (t, 8H, OCH_2, ^3J = 6.2); 7.02 (s, 2H, CH); 7.04 (s, 2H, CH); 7.58 (s, 2H, CH); 7.62 (8H, AA'BB'); 7.71 (s, 2H, CH). **^{13}C NMR** (100 MHz, $CDCl_3$): δ 14.2, 14.3 (CH_3); 22.80, 22.84, 25.0, 25.87, 25.93, 29.38, 29.44, 31.7, 31.8 (CH_2); 69.7, 69.8 (OCH_2); 88.8, 90.6, 92.2, 93.5 (C≡C); 111.6, 113.4, 114.3 (C_q); 116.5, 117.0 (C_t); 118.7 (C_q); 121.2 (C_t); 122.4, 128.5 (C_q); 129.7, 132.1, 132.2 (C_t); 133.8, 137.5, 153.7, 154.9 (C_q). **EA** [%]: $C_{68}H_{68}N_2O_4S_2$ Calc. for C 78.43, H 6.58, N 2.69 Found C 78.11, H 6.60, N 2.63; **FD-MS:** *m/z* [%]: 1040.5 (100, M^+); 1041.5 (79, $[M+1]^+$).

2,7-bis-{4-[4-(3-cyanophenylethynyl)-2,5-bis(hexyloxy)phenyl]ethynylphenyl}benzo[2,1-b:3,4-b']dithiophene (2b): **^{1}H NMR** (400 MHz, $CDCl_3$): δ 0.91 (t, 6H, CH_3, ^3J = 7.0); 0.93 (t, 6H, CH_3, ^3J = 7.0); 1.35 - 1.45 (m, 16H, CH_2); 1.50 - 1.64 (m, 8H, CH_2); 1.82 - 1.94 (m, 8H, CH_2); 4.052 (t, 4H, OCH_2, ^3J = 6.4); 4.055 (t, 4H, OCH_2, ^3J = 6.2); 7.02 (s, 2H, CH); 7.04 (s, 2H, CH); 7.47 (m, 2H, CH); 7.58 (s, 2H, CH); 7.61 (m, 2H, CH); 7.71 (s, 2H, CH); 7.74 (m, 2H, CH); 7.80 (m, 2H, CH). **^{13}C NMR** (100 MHz, $CDCl_3$): δ 14.2, 14.3 (CH_3); 22.82, 22.84, 25.90, 25.93, 29.38, 29.43, 31.7, 31.8 (CH_2); 69.7, 69.8 (OCH_2); 88.6, 88.7, 92.2, 92.6 (C≡C); 113.0, 113.4, 114.1 (C_q); 116.6, 117.0 (C_t); 118.2 (C_q); 121.1 (C_t); 122.4, 125.2 (C_q); 129.4, 129.7, 131.5 (C_t); 133.8 (C_q); 134.9, 135.7 (C_t); 137.5, 153.8, 154.0 (C_q). **EA** [%]: $C_{68}H_{68}N_2O_4S_2$ Calc. for C 78.43, H 6.58, N 2.69, S 6.16 Found C 77.85, H 6.51, N 2.90, S 5.87; **FD-MS:** *m/z* [%]: 1040.9 (100, M^+); 1041.9 (72, $[M+1]^+$).

2) Schlieren textures of nematic phases

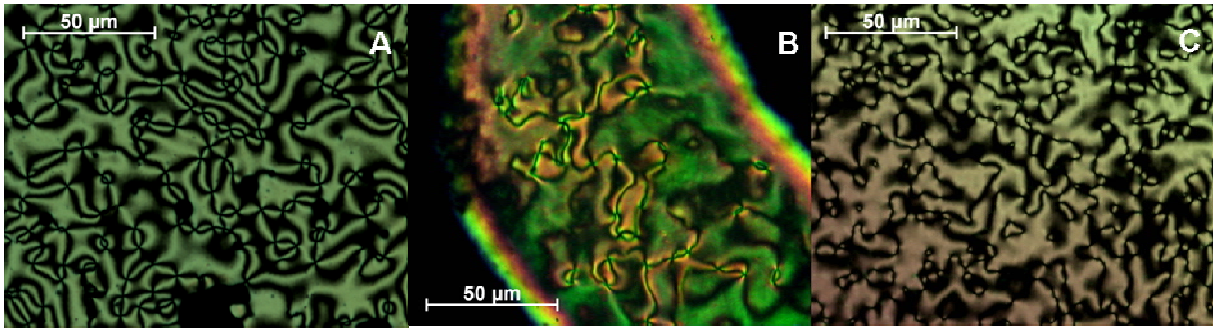

Figure S1. Typical Schlieren textures of the nematic phases of **1b** at 77 °C (A), of **1c** at 50 °C (B) and **2b** at 85 °C (C) between crossed polarisers.

3) Conoscopy on tilted multi domains and mono domains with sample tilt

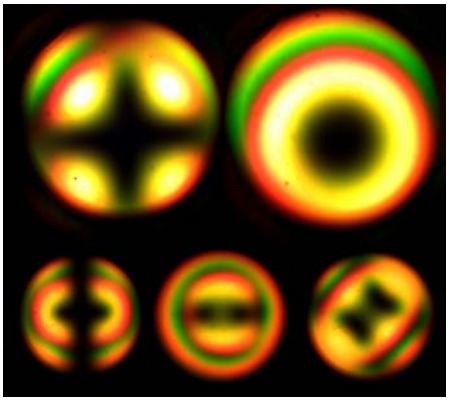

Figure S2. Upper row: Conoscopic images of the tilted uniaxial multi domain area of **1c** in cell (2) at 60 °C. Left: Conoscopic cross; Right: optical axis visualised with the circular polariser. Bottom row: Conoscopic images of the same sample at rt. Normal (left) and diagonal (right) position and optical axes visualised with a circular polariser at normal position (middle). The images were centred by tilting the sample by 6° along the rubbing direction.

4) Biaxial director fields of uniaxial phases

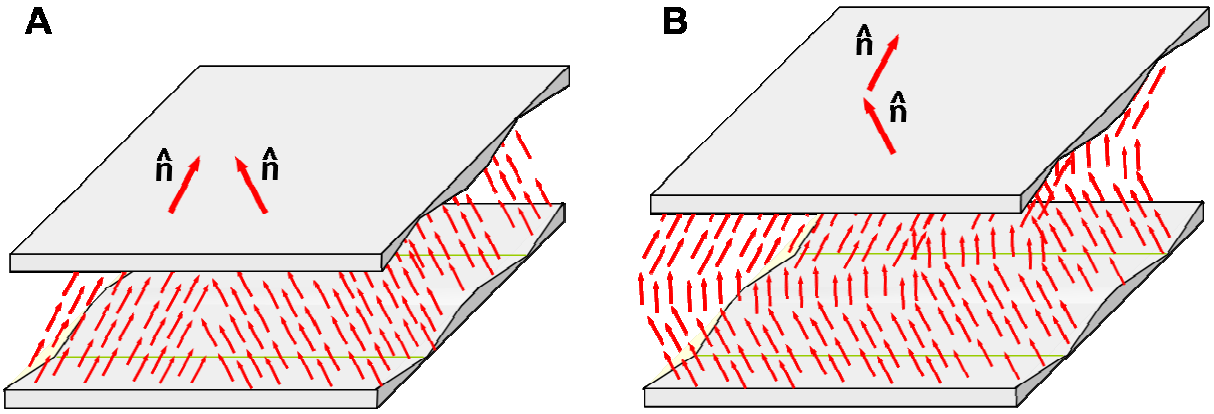

Figure S3. Possible director fields generated from uniaxial phases, which implies a biaxial answer by polarised optical microscopy. Case (A): Two tilted uniaxial nematic phases. Case (B): Different tilt induced by the lower and upper surfaces.

Two biaxial director fields were suggested by Y. Galerne to pretend biaxial order from uniaxial nematic phase.[8] In case (A) a symmetrical conoscopic image with two optical axes can only be obtained when the objective is placed in the middle between the two domains. A single tilted uniaxial nematic phase results only in one off-centred optical axis. Case (B) may be realised easily in parallely rubbed LC cells and biaxiality should be observed all over the monodomain. However, tilt is strongest at the interfaces and reduces versus the middle of the cell. Therefore a very thick cell should reveal a large part with a homeotropically aligned, uniaxial material. The latter reduces the splitting of the isogyres and the optical axes. Thus in thick cells a strong reduction of the splitting should be expected.

[8] Y. Galerne, *Mol. Cryst. Liq. Cryst.* **1998**, *323*, 211.

5) Orthoscopy and Conoscopy of compound 2b in cell (1)

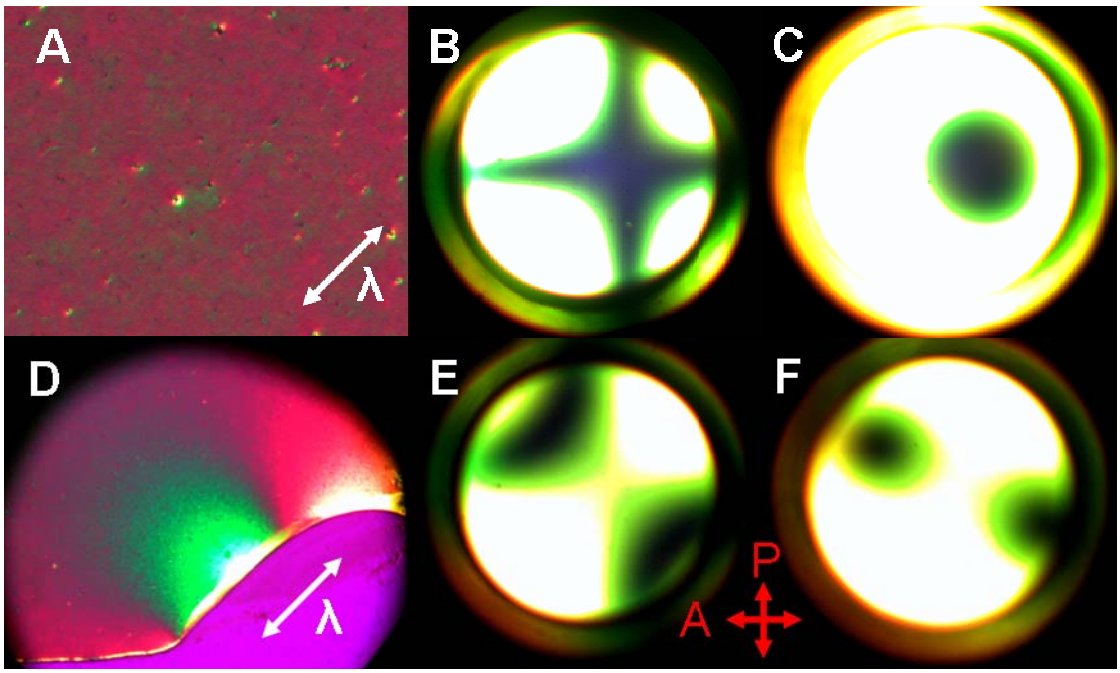

Figure S4. POM of **2b** at T_{NI}-T = 1.3 °C in cell (1) between crossed polarisers (A and P; red arrows). A: Multi domain structure observed applying the λ compensation plate. In the green part the largest refractive index of the sample adds on the largest refractive index of the λ plate (white arrow), indicating that the molecular long axes are oriented parallel with the same direction. B,C: Conoscopy without and with circular polariser indication the uniaxial nature of the multi domain structure. D: Mono domain (green) at the LC/air interface. E-F: Conoscopy on the mono domain reveals its biaxial character. Diagonal position (E), image using the circular polariser showing the two optical axes (F).

6) X-Ray scattering

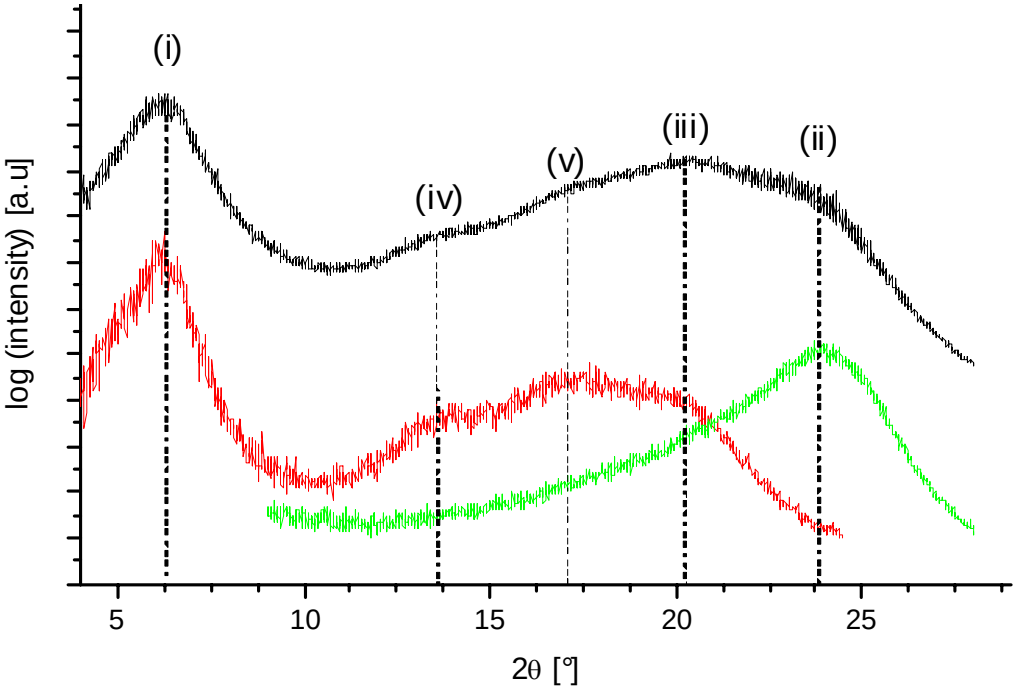

Figure S5. X-ray scattering of a magnetic field aligned sample of **1b** at 50 °C. Black: Integration over the whole azimuth (360°). Red: Integration along the equator. Green: Integration along the meridian. Distances d and correlation lengths ξ/d are (i) d(i) =14.0 Å (ξ/d(i) = 4), (ii) d(ii) =3.7 Å (ξ/d(ii) = 10)), Halo d(iii) =4.4 Å (ξ/d(iii) = 4/8), d(iv) =6.6 Å (ξ/d(iv) = 8), d(v) =5.2 Å (ξ/d(v) = 5).

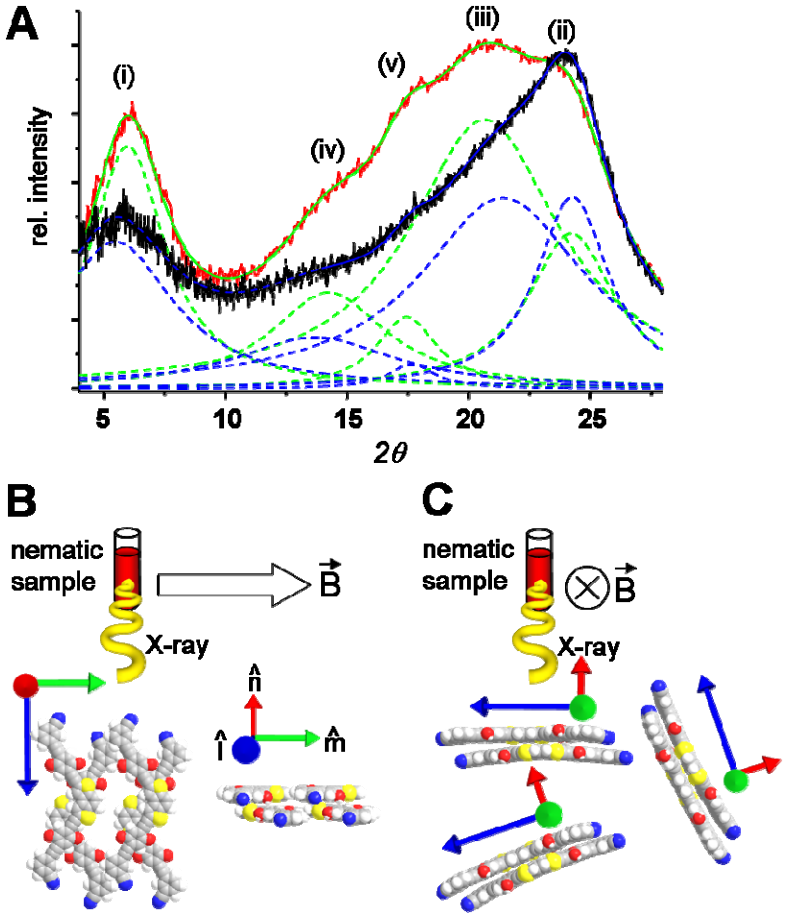

Figure S6. X-ray scattering of a magnetic field aligned sample of **1c** at 30 °C (A). Red: Integration over the whole azimuth angles (0-360°) of the diffraction pattern obtained with the X-ray beam orthogonal the applied magnetic field. Single fit curves (dashed) and the sum of the fit curves (solid) in green. Black: Integration over the whole azimuth angles (0-360°) of the diffraction pattern obtained with the X-ray beam parallel to the applied magnetic field. Single fit curves (dashed) and the sum of the fit curves (solid) in blue. B: Orthogonal orientation of the magnetic field aligned sample with respect to the X-ray beam and domain orientations resulting in peaks (i) – (v). C: Parallel orientation of the magnetic field aligned sample with respect to the X-ray beam and domain orientations resulting in increasing intensity of peaks (ii) relative to (i), (iv) and (v).

The diffraction pattern for magnetic field aligned compound **1c** in **Figure S6** clearly evidences, that the molecules are oriented in the magnetic field. The diffraction pattern recorded orthogonal (red) to the direction in which the magnetic field was applied distinguish significantly from the pattern obtained parallel (black) to the magnetic field. All peaks originating from the orientational ordered molecules along the director **m**, i.e. the apex bisector of the molecule (peaks (i), (iv), (v)) possess a significant decreased intensity for the black curve relative to the red curve. Thus mesogens orient preferentially with there bisector parallel to the magnetic field. The same alignment has been found for fluorenone mesogens in their nematic phase.[9,10] Thus these mesogens distinguish from the alignment of calamitic or different banana shaped compounds.[11]

[9] M. Lehmann, Ch. Köhn, C. Cruz, J. L. Figueirinhas, G. Feio, R. Dong, *Chem. Eur. J.* 2010, **16**, 8275.
[10] J. L. Figueirinhas, G. Feio, C. Cruz, M. Lehmann, Ch. Köhn, R. Dong, *J. Phys. Chem.* 2010, **133**, 174509.
[11] V. Domenici, C. A. Veracini, K. Fodor-Csorba, G. Prampolini, I. Cacelli, A. Lebar, B. Zalar, *ChemPhysChem* 2007, **8**, 2321 – 2330.

7) Model of the mesogen orientation in a LC cell

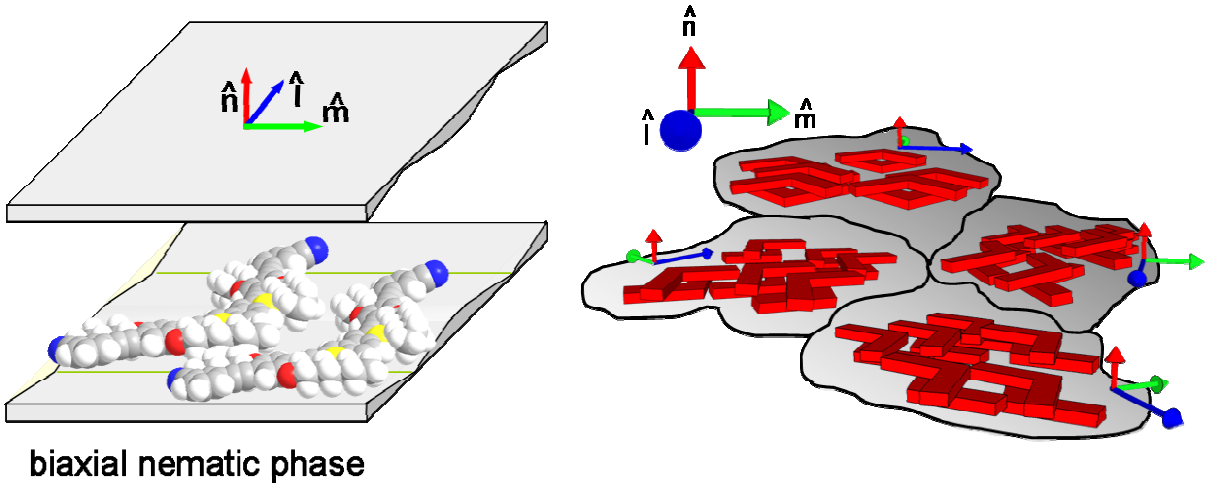

Figure S7. Schematic drawing of the biaxial orientation of molecules in the nematic phase (left) and the multi domain structure (right).

Conoscopy revealed that the nematic phase of **1c** is optically negative, i.e. the largest refractive index must be parallel to the surface. This can be accomplished when directors **n** or **m** are perpendicular oriented to the glass surfaces. However, in the later case, the optical axes would be parallely oriented with the surface and consequently the optical axes would not be visible. Since in cells (1) and (2) the optical axes were visualised by application of the circular polariser, the director **n** must be perpendicular to the glass sheets as shown in Figure S7, i.e. the π-faces of the molecules are parallel with the surface.